ADVANCED HEALTHCARE MATERIALS
www.advhealthmat.de

Glepaglutide-Loaded Foam for the Induction of Mucosal Healing in the Treatment of Inflammatory Bowel Disease

*Wunan Zhang, William Van den Bossche, Hafsa Yagoubi, Espoir K Kambale, Khadija Wahni, Tanya Saxena, Léo Guilbaud, Tom G. Moreels, Joris Messens, and Ana Beloqui**

Glucagon-like peptide 2 (GLP-2) stimulates intestinal growth, repairs mucosa, and enhances epithelial integrity but has a short half-life (7 min). Glepaglutide (GL), a GLP-2 analog with an extended half-life (50 h), is currently undergoing clinical trials for patients with short bowel syndrome. GL requires subcutaneous injection, which poses challenges for potential patient compliance. To address this challenge, GL was loaded into a rectal foam formulation using CO_2 as a permeation enhancer to combine both the local and systemic effects of the GLP-2 analog. In a dextran sodium sulfate (DSS)-induced colitis model, the GL-loaded foam (GLF) significantly mitigated the severity of colitis. GLF facilitated mucosal healing, as evidenced by colonoscopy images, increased plasma markers of mucosal healing, and increased crypt depth. To evaluate GL absorption in the colon, fluorescein dextran 4K (FD 4K) was employed. The foam formulation improved macromolecule absorption in the colon, with fast recovery of enhanced permeation that dissipated after 4 h. This study highlights GLF as a promising formulation for GL administration, balancing systemic and local anti-inflammatory effects.

1. Introduction

Glucagon-like peptide 2 (GLP-2), a 33-amino acid peptide, is secreted by enteroendocrine L cells located in the intestine and colon.[1,2] It acts as a pleiotropic regulator of intestinal health, exerting both direct and indirect effects on various aspects of intestinal function.[3] It directly binds to GLP-2 receptors, stimulating cell proliferation and reducing apoptosis by increasing the production of cyclic adenosine monophosphate (cAMP).[1,3,4] GLP-2 indirectly enhances intestinal barrier function and has anti-inflammatory properties.[5,6] These effects have spurred research into the therapeutic efficacy of GLP-2 for the treatment of inflammatory bowel disease (IBD), which is characterized by damage to the colon mucosa, an impaired epithelial barrier, and relapse-remitting chronic inflammation.[7–9] However, the clinical use of native GLP-2 is limited because of its rapid breakdown by dipeptidyl peptidase-4

W. Zhang, W. Van den Bossche, H. Yagoubi, E. K Kambale, T. Saxena, L. Guilbaud, A. Beloqui
UCLouvain, Université catholique de Louvain
Louvain Drug Research Institute
Advanced Drug Delivery and Biomaterials
Brussels 1200, Belgium
E-mail: ana.beloqui@uclouvain.be

K. Wahni, J. Messens
VIB-VUB Center for Structural Biology
Brussels 1050, Belgium

K. Wahni, J. Messens
Brussels Center for Redox Biology
Brussels 1050, Belgium

K. Wahni, J. Messens
Structural Biology Brussels
Vrije Universiteit Brussel
Brussels 1050, Belgium

T. G. Moreels
Institute of Experimental and Clinical Research
Laboratory of Hepato-Gastroenterology
UCLouvain, Université Catholique de Louvain
Brussels 1200, Belgium

T. G. Moreels
Cliniques universitaires Saint-Luc
Department of Gastroenterology & Hepatology
Brussels 1200, Belgium

A. Beloqui
WEL Research Institute
Avenue Pasteur, 6, Wavre 1300, Belgium

The ORCID identification number(s) for the author(s) of this article can be found under https://doi.org/10.1002/adhm.202403497

DOI: 10.1002/adhm.202403497

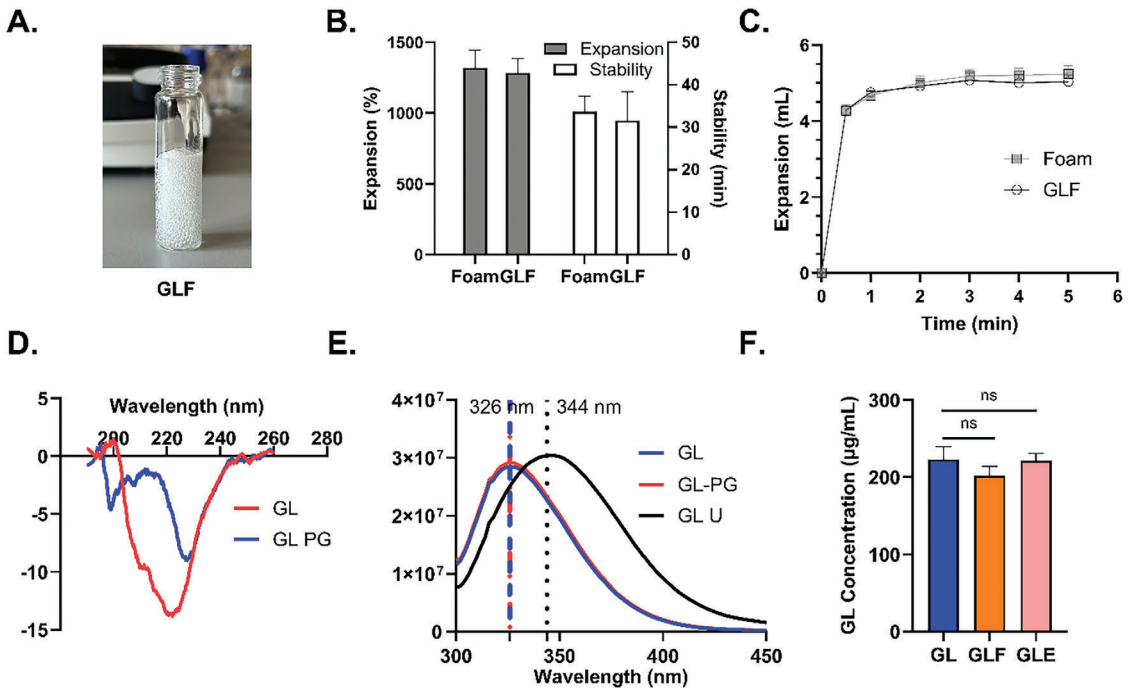

Figure 1. Characterization and stability of GLF. A) Image of the foam expanded in a vial. B) Expansion and stability of the foam and GL-loaded foam (GLF) (n = 6). C) Expansion kinetics of foam and GLF (n = 6). D) Mean CD spectra of GL before gassing (GL) and GL after gassing (GL PG) (n = 3). E) Mean intrinsic fluorescence spectra of GL before gassing (GL), GL after gassing (GL PG) and unfolded GL (GL U). The maximum wavelengths are marked with lines of the corresponding color (n = 3). F) GL concentrations before gassing and in the final formulations (n = 9). Statistical analysis was conducted using Student's *t* test (B) or one-way ANOVA followed by Tukey's multiple comparison test (F). The results are presented as the mean ± standard error of the mean (SEM) (B, C&F) or as the mean only (D&E).

(DPP-4), with an elimination half-life of only 7 min in healthy individuals.[10] This challenge has been addressed by developing GLP-2 analogs resistant to DPP-4 degradation through the substitution of the alanine at position 2.[11] Glepaglutide (GL), a modified form of GLP-2, features nine amino acid substitutions (including substitution of alanine at position 2) and a C-terminal tail with six lysine residues, significantly extending its elimination half-life to up to 50 h in humans.[12,13] Currently, GL has completed phase 3 clinical trials (NCT04991311, NCT03690206) for its use in the treatment of short bowel syndrome (SBS).[14] The primary delivery method in clinical reports of GL remains subcutaneous injection, which can impede patient compliance. Consequently, exploring novel and less invasive drug delivery systems could substantially increase its therapeutic potential.

Despite several studies exploiting the use of GLP-2 peptides in IBD treatment,[15,16] to our knowledge, the potential of local administration of GL in IBD therapy has not been explored. In a recent study from our group, we demonstrated that rectally administered in situ foam, which uses CO_2 as a permeation enhancer, could efficiently improve the therapeutic effect of antibody fragments by enhancing colon absorption and prolonging drug retention at the inflamed site. We expect that this formulation could similarly enhance the therapeutic efficacy of GL via noninvasive local administration.[17]

The effect of the gas generation process on the stability of GL was tested via various techniques, including circular dichroism (CD), intrinsic fluorescence, and degradation analysis. The efficacy of the formulation was assessed in an acute colitis mouse model induced by dextran sodium sulfate (DSS), with GL administered subcutaneously (s.c.) as a positive control. Both the local anti-inflammatory effects and the systemic intestinotrophic effects were assessed. To evaluate the permeation enhancement effect of the formulation in vivo, fluorescein dextran with a molecular weight similar to that of GL (FD 4K) was incorporated into foam. Its absorption was studied in colitis mice, whereas the recovery of permeability enhancement induced by the foam was studied in healthy mice. This study provides with a novel alternative for the delivery of GLP-2 analogs in IBD treatment.

2. Results

The foam was prepared by combining the acidic and basic components in equal volumes (1:1 ratio), achieving successful expansion within a cylindrical container, as depicted in **Figure 1A**. Subsequently, GL was incorporated into the foam formulation to assess its impact on two key parameters: foam expansion volume and foam stability. As demonstrated in Figure 1B, the foam expanded to 5.28 mL, whereas GLF expanded to 5.13 mL (Figure 1B). Foam stability was evaluated by measuring the duration it remained intact in a scaled Falcon tube at 37 °C, with the foam persisting for 33.6 min compared with 31.6 min for GLF (Figure 1B). These results revealed no significant differences, implying that the peptide does not influence the foam characteristics. Both formulations exhibited comparable expansion kinetics, with initial rapid expansion at the onset of the foaming process

(Figure 1C). Maximum expansion was attained after 2 min, indicating that the foam expansion was not immediate.

The stability of GL in the basic preformulation solution (utilized for both GLF and GLE) was assessed by monitoring changes in GL concentration over time, as shown in Figure 1 (Supporting Information). The results indicated that GL remained stable in the basic preformulation solution for up to 3 months at 4 °C.

To determine whether GL can withstand the gassing process, CD and intrinsic fluorescence analyses were conducted to assess the stability of GL after gassing. As illustrated in Figure 1D, the CD spectrum of GL after gassing (GL PG) differed from that of the GL prior to the gassing process, indicating a significant loss in secondary structure. Specifically, the α-helix content of GL decreased from 36.9% in the basic prefoam formulation to 14.4% following gassing. Interestingly, the intrinsic fluorescence spectrum of GL remained unchanged before and after gassing, with no redshift in the maximum emission wavelength observed; this suggests that while even GL remains unfolded at the site induce intrinsic fluorescence, more than half of the secondary structure is lost after gassing (Figure 1E).

Further stability assessments involved measuring the GL concentration in GLF both before and after the gassing process. To determine whether the foaming excipients are responsible for stabilizing the peptide, an effervescent formulation (GLE) was utilized for comparison. As depicted in Figure 1F, there was no decrease in the GL concentration in either GLF or GLE compared with the GL concentration in the basic preformulation solution (before gassing). This finding indicates that the gassing process does not lead to GL degradation and that foaming excipients do not contribute to peptide stabilization.

To demonstrate its therapeutic potential in mice, the efficacy of GLF was evaluated in a DSS-induced colitis mouse model, with the subcutaneous injection of GL (GLsc) serving as a benchmark. Notably, a previous study showed that an effervescent formulation (foam without foaming excipients) enhanced colon macromolecule absorption, suggesting the potential for improved systemic effects. To assess whether foaming excipients are essential for IBD treatment, GLE was also administered for comparison. Additionally, rectally administered GL solution (GLS) was used to assess the impact of the formulation on the therapeutic effect of locally administered GL. The construction of the acute colitis model, along with the GL treatment administration schedule, is illustrated in **Figure** 2A. The correlation of weight loss progression with disease development is presented in Figure 2B. Notably, GLsc was the only treatment that effectively mitigated weight loss in the mice, a trend not observed in any other treatment groups.

Colon inflammation is characterized by increased colon weight, reduced colon length, and consequently, a decreased colon length-to-weight ratio. Although foam, GLsc, and GLF significantly reduced colon weight (Figure S2, Supporting Information), none of these treatments effectively preserved colon length (Figure S2, Supporting Information). As a result, none of the treatments improved the colon length-to-weight ratio (Figure 2C).

The murine endoscopic index of colitis severity (MEICS) demonstrated that both GLsc and GLF significantly reduced the severity of colitis (colitis vs GLF, $p = 0.0215$; colitis vs GLsc, $p = 0.0005$), resulting in a more transparent colon mucosa (Figure 2D). These results validated that locally administered foam could provide comparable efficacy to that of systemically administered GL to induce mucosal healing. However, GLS and GLE only exhibited a decreasing trend in MEICS without significant differences, suggesting that these two formulations could not provide sufficient therapeutic effects.

Histological analysis of H&E-stained slides further confirmed that both GLsc and GLF substantially reduced colitis severity compared with that in the colitis control group ($p = 0.048$ and $p = 0.0349$, respectively, *t*-test) (Figure 2E). However, these significant differences were not detected using one-way ANOVA.

In summary, although GLsc was the only treatment used to effectively mitigate weight loss in colitis-afflicted mice, GLF exhibited comparable therapeutic efficacy across the other evaluated parameters (MEICS and histology).

Microscopic markers were further evaluated to substantiate the anti-inflammatory effects of the formulations (**Figure** 3). Proinflammatory cytokines were measured in the distal colon, the region with the most severe inflammation. The TNF-α levels in the colon mucosa were significantly reduced by both GLS and GLsc treatments (56.8% and 55.8%, respectively, compared with those in the colitis mice) (Figure 3A, GLS vs colitis, $p = 0.0237$; GLsc vs colitis, $p = 0.0235$). GLE treatment also tended to lower TNF-α concentrations (48.5% compared with colitis mice), showing reduced concentrations comparable to healthy mice (healthy vs GLE; $p > 0.05$).

However, a significant reduction in the mucosal KC/GRO concentration was not observed even between healthy mice and mice with colitis (healthy vs colitis; $p > 0.05$), although GLS and GLsc were associated with a reduction in the mean KC/GRO concentration (Figure 3B).

GLS and GLF significantly decreased the IL-6 concentration in the colon mucosa (GLS vs colitis, $p = 0.0267$; GLF vs colitis, $p = 0.0225$), whereas GLsc and GLE also yielded IL-6 levels comparable to those in healthy mice (GLsc vs healthy, $p > 0.05$; GLE vs healthy, $p > 0.05$). However, the reductions (53.5% and 54.5%, respectively) were not significant compared with those in the colitis group. Notably, GLF exhibited the most pronounced decrease, with an 80% reduction in IL-6 levels, whereas GLS demonstrated a significant decrease exceeding 70%.

Moreover, GLsc, GLF, and GLE significantly lowered the IL-1β level by more than 60% (GLsc vs Colitis, $p = 0.0113$; GLF vs Colitis, $p = 0.0176$; GLE vs Colitis, $p = 0.0173$), whereas GLS did not significantly reduce (45.5%) the IL-1β level in the colon mucosa.

MPO activity was assessed to evaluate neutrophil infiltration. Compared with the colitis model mice, the healthy control mice presented significantly ameliorated MPO activity (51%). GLsc, GLS, and GLF all demonstrated efficacy in reducing MPO activity to levels comparable with those of the healthy group (36.4, 42.0% and 32.3%, respectively) (GLsc vs healthy, $p > 0.05$; GLS vs healthy, $p > 0.05$; GLF vs healthy, $p > 0.05$), with a similar decrease observed across these formulations.

In summary, both locally and systemically administered GL exhibited therapeutic efficacy by reducing the levels of proinflammatory cytokines and MPO activity. Locally administered GLS and GL in CO_2-containing formulations showed significant potential to alleviate disease severity. In particular, GLF markedly reduced the levels of inflammatory markers such as IL-6, IL-1β, and MPO, highlighting its potential as an efficient alternative treatment for systemically administered GL (GLsc).

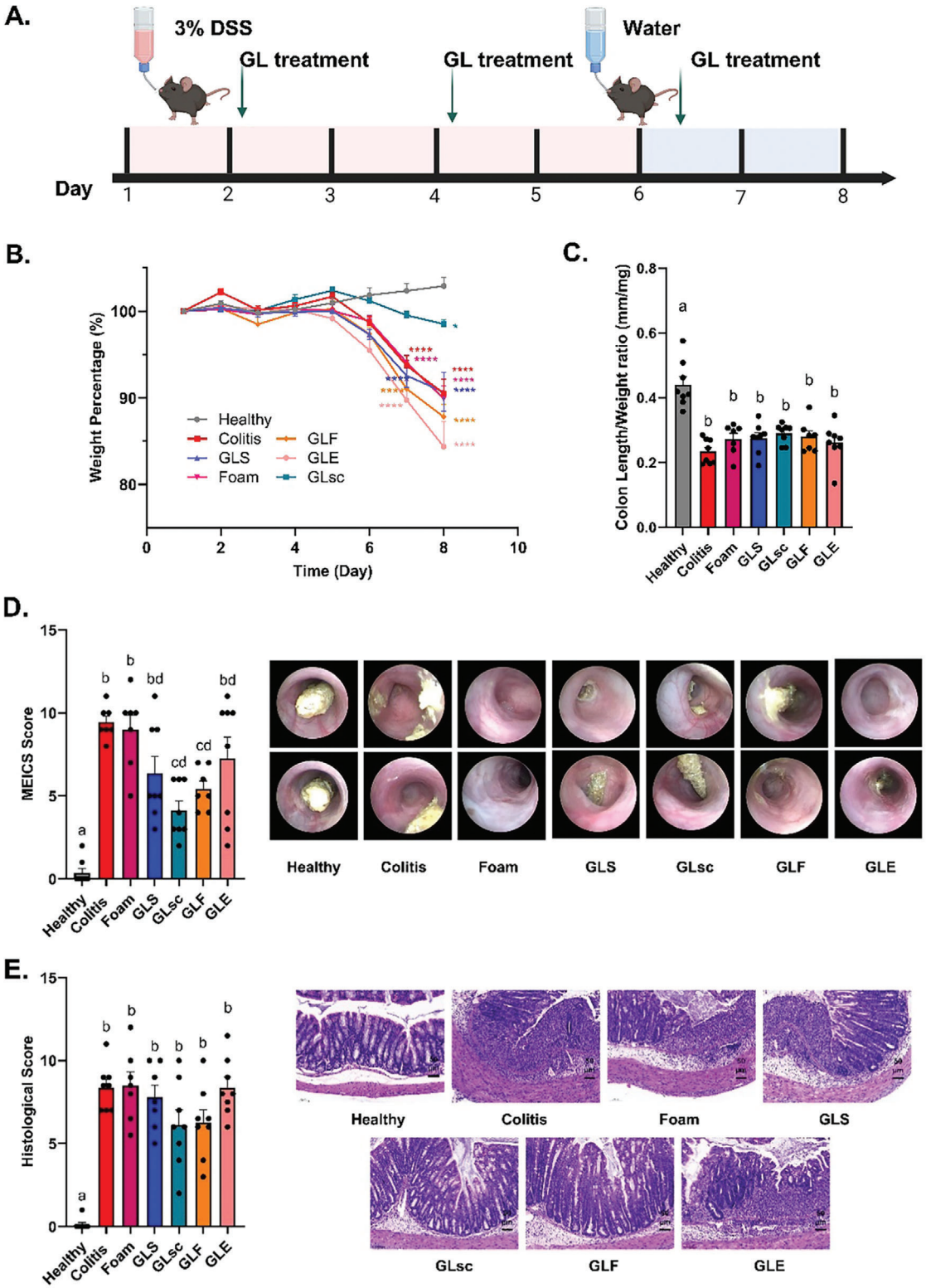

Figure 2. In vivo efficacy evaluation of the GL-loaded formulation in an acute colitis model induced by DSS. A) Scheme of the DSS-induced colitis model and dosing in which GL was administered at Days 2, 4, and 6. B) Percent weight loss of the mice (n = 7–8). C) Colon weight-to-length ratio (n = 7–8). D) MEICS scores (n = 7–8) and representative images per group. E. Histological analysis (n = 7–8) and representative images per group; the scale bar represents 50 µm. Statistical analysis was performed using two-way ANOVA (B) or one-way ANOVA followed by Tukey's multiple comparison test (C–E). Superscript letters (a, b, ab, etc.) represent the results of Tukey's multiple comparison. These letters are a shorthand to show significant differences between the groups. The data are presented as the means ± SEMs.

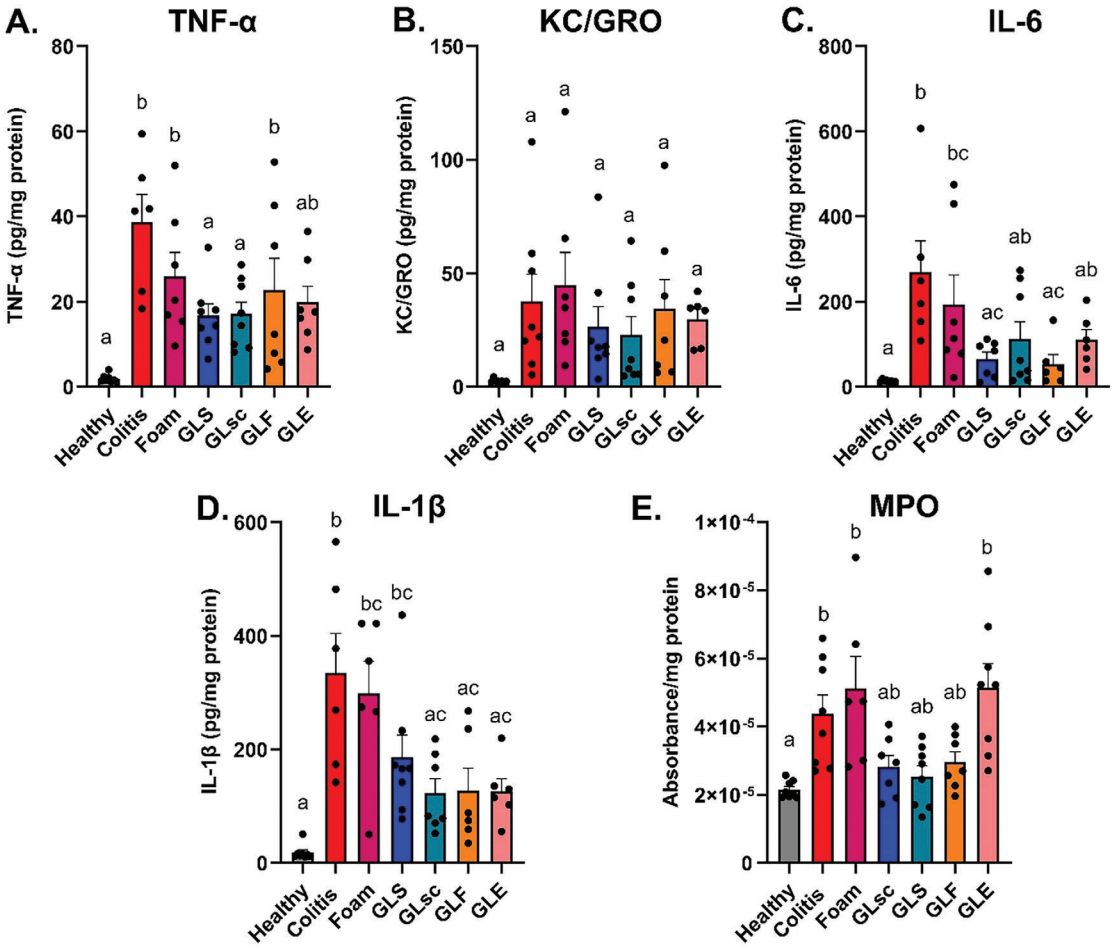

Figure 3. Proinflammatory cytokines and MPO activity in an acute murine colitis model. A) TNF-α concentration in the colon (n = 6–8). B) KC/GRO concentration in the colon (n = 6–8). C) IL-6 concentration in the colon (n = 6–8). D) IL-1β concentration in the colon (n = 6-8). E) MPO activity in the colon (n = 6–8). Statistical analysis was conducted via one-way ANOVA followed by Tukey's multiple comparison test. Superscript letters (a, b, ab, etc.) represent the results of Tukey's multiple comparison. These letters are a shorthand to show the significant differences between groups. The data are presented as the means ± SEMs.

The intestinotrophic effect of the GLP-2 analog is closely related to its mucosal healing effect and requires absorption for locally delivered GL. Thus, the intestinotrophic effect and systemic mucosal healing marker concentrations were further assessed, as shown in **Figure 4**. The empty weight of the intestines was measured to evaluate the intestinotrophic effect (Figure 4A). Systemically administered GL increased the intestinal weight by 1.5-fold, whereas locally administered formulations had no effect. Notably, DSS alone had no effect on intestinal weight in the acute model.

The level of plasma citrulline, a marker of mucosal healing secreted by enterocytes exclusively in the small intestine, was also measured (Figure 4B). GLsc, GLF, and GLE demonstrated citrulline levels comparable to those of healthy mice ($p > 0.05$). More importantly, compared with foam without GL, GLsc, GLF, and GLE significantly increased plasma citrulline concentrations by 200%, 199.5%, and 184.2%, respectively (GLsc vs foam, p = 0.0236; GLF vs foam, p = 0.0075; GLE vs foam, p = 0.0058), indicating that these formulations promote mucosal healing. Notably, locally administered GL (GLS) failed to improve plasma citrulline levels, suggesting that GL-loaded formulations containing CO_2 can induce systemic effects and promote mucosal healing, comparable to local administration alone.

The intestinotrophic effect of GLP-2 was demonstrated by the increase in villus height and crypt depth, which were observed in the ileum and jejunum. Interestingly, DSS-treated mice presented significant decreases in both villus height and crypt depth in the jejunum (Figure 4C,D). Compared with the colitis group, only the GLsc group presented a 208% greater villus height (Figure 4C). Although GLS, GLF, and GLE showed villus heights comparable to those of healthy mice (GLS, GLF, and GLE vs healthy, $p > 0.05$), the improvements were not statistically significant compared with those of colitis mice (Figure 4C). In terms of crypt depth, GLF and GLE mitigated the reduction observed in the colitis mice, with crypt depths similar to those of the healthy mice (increased by 125% and 120% compared with those of the colitis group, respectively; GLF versus colitis, $p < 0.0001$; GLE vs colitis, p = 0.002). GLsc exhibited the most potent effect on promoting crypt depth (increase of 136% compared with that of the colitis group), with values significantly greater than those of not

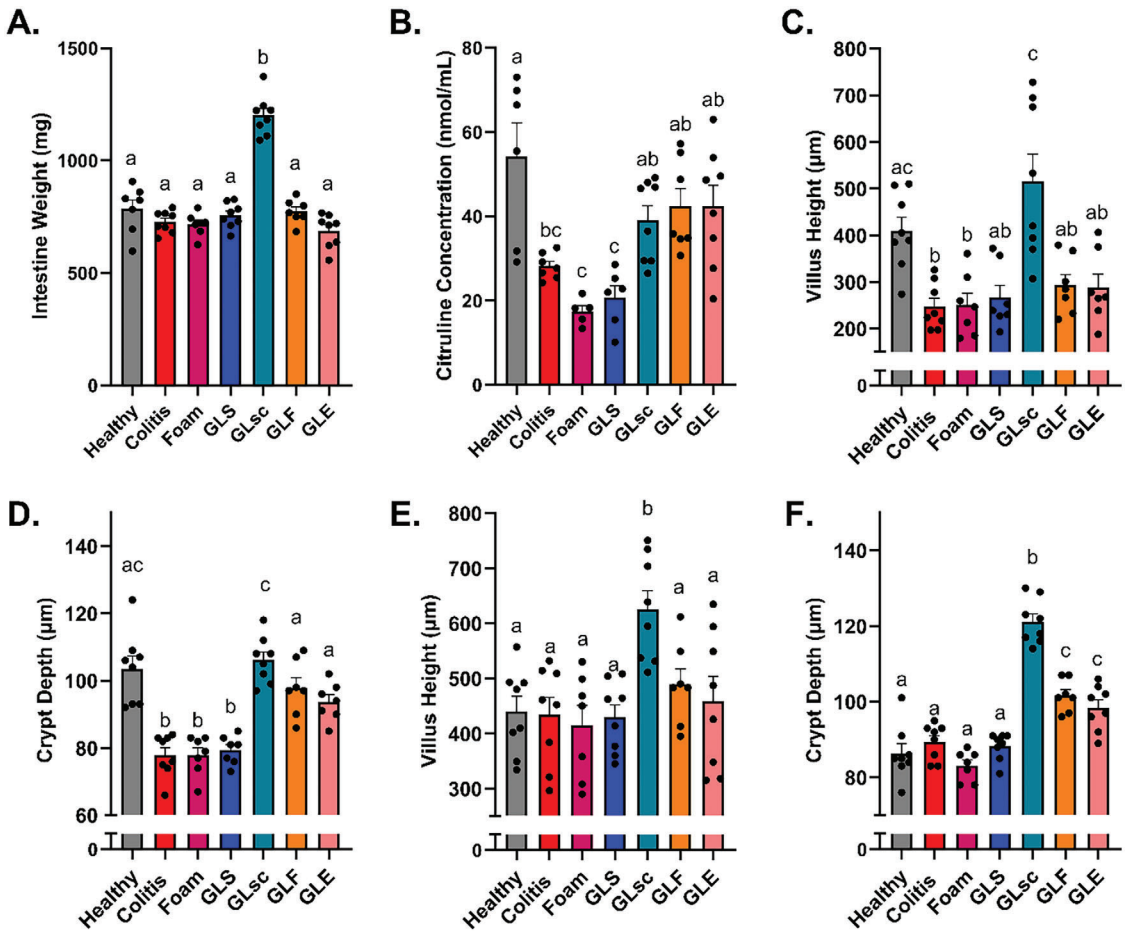

Figure 4. Systemic effect of locally administered GL. A) Intestine weight length (n = 6–8). B) Plasma citrulline concentration (n = 6–8). C) Villus height in the jejunum (n = 7–8). D) Crypt depth in the jejunum (n = 7–8). E) Villus height in the ileum (7–8). F) Crypt depth in the ileum (n = 7–8). Statistical analysis was conducted via one-way ANOVA followed by Tukey's multiple comparison test. Superscript letters (a, b, ab, etc.) represent the results of Tukey's multiple comparison. These letters are a shorthand to show significant differences between the groups. The data are presented as the means ± SEMs.

only the colitis group but also those of the GLF and GLE groups (Figure 4D, GLsc vs colitis, $p < 0.0001$; GLsc vs GLE, $p = 0.0274$).

In the ileum, DSS treatment did not significantly affect the villus height or crypt depth (healthy vs colitis, $p > 0.05$). Similar to the observations in the jejunum, only GLsc significantly increased the villus height by 144.3% (GLsc vs Colitis, $p = 0.0022$). The trend in crypt depth in the ileum was consistent with that in the jejunum. Compared with the colitis mice, the GLF and GLE groups presented significantly greater crypt depth (114% and 110%, respectively) (GLF vs colitis, $p = 0.0009$; GLE vs colitis, $p = 0.0215$), whereas the GLsc group presented the most pronounced increase in crypt depth (135%; GLsc vs colitis, $p < 0.0001$). Notably, all treatment groups presented increased crypt depth compared with that of healthy mice, except for GLS (GLF vs healthy, $p < 0.0001$; GLE vs healthy, $p = 0.0007$; GLsc vs healthy, $p < 0.0001$).

These findings underscore that GL demonstrates an intestinotrophic effect when it is administered systemically. Gas-containing formulations, such as GLF and GLE, can produce similar, albeit milder, effects when applied locally. In contrast, locally administered GL solution does not induce a systemic response, suggesting that gas-containing formulations enhance GL absorption and thereby facilitate its systemic impact.

Locally administered GLF and GLE induce systemic effects similar to those of GLsc, indicating enhanced absorption of GL in the colon. To further elucidate the in vivo behavior of these formulations, FD 4K was used as a surrogate to measure the systemic concentration of macromolecules following local administration of CO_2-containing formulations. FD 4K solution (FDS), FD 4K-loaded foam (FDF), and FD 4K-loaded effervescent system (FDE) were administered to mice with colitis (**Figure** 5A). Both FDF and FDE significantly increased the systemic FD 4K concentration within 15 min postrectal administration (FDF vs FDS, $p < 0.0001$; FDE vs FDS, $p = 0.0002$), whereas FDS resulted in only minimal plasma FD 4K levels, comparable to those of blank plasma.

To investigate the permeation enhancement effect induced by the foam formulation, a permeation enhancement recovery experiment was conducted in healthy mice. FDS and FDF were administered rectally to the mice. Foam without FD 4K was administered rectally, followed by FD 4K in solution after 4 h (Figure 5C). The plasma changes in FD 4K are shown in

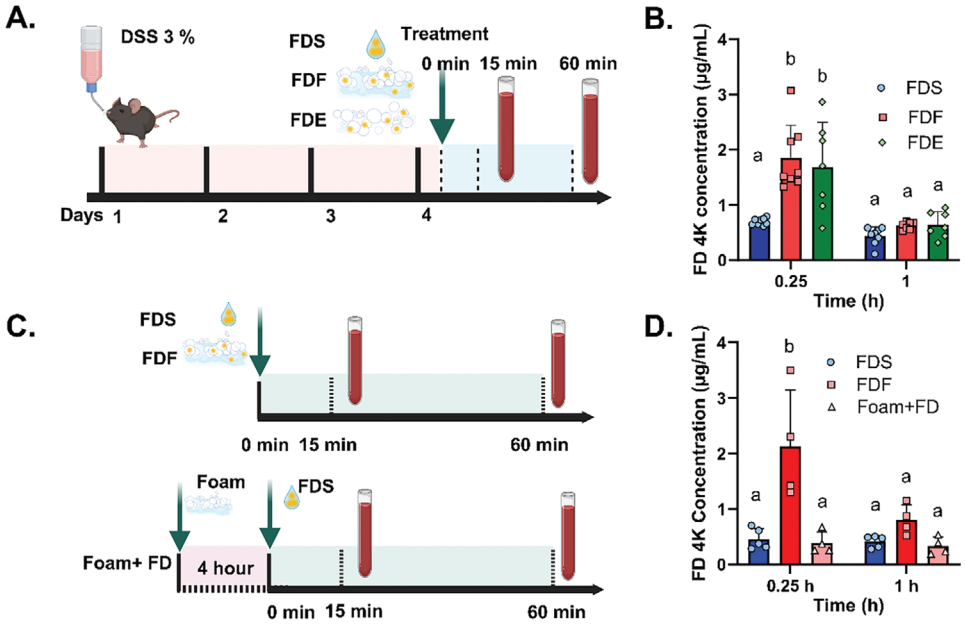

Figure 5. CO_2-enhanced macromolecule plasma concentrations. A) Scheme of administration of FD 4K formulations in mice with colitis induced by 3% DSS. B) Plasma FD 4K concentration (n = 7–8). C) Illustrative sketch of FD 4K formulation administration in healthy mice. D) Plasma concentration of FD 4K in healthy mice (n = 4–5). Statistical analysis was conducted using two-way ANOVA followed by Tukey's multiple comparison test. Superscript letters (a, b, ab, etc.) represent the results of Tukey's multiple comparison. These letters are a shorthand to show significant differences between the groups. The data are presented as the means ± SEMs.

Figure 5D. Consistent with the results in colitis mice, FDS exhibited minimal absorption, whereas FDF significantly increased plasma FD 4K levels 15 min postadministration (FDF vs FDS, $p < 0.0001$). Notably, the permeation enhancement effect of the foam formulation dissipated after 4 h, with no increase in the plasma FD 4K concentration observed.

These findings confirmed that CO_2-containing formulations effectively act as permeation enhancers when coadministered with macromolecules to induce systemic effects. Interestingly, this permeation effect is transient and dissipates after 4 h.

3. Discussion

We have developed an in situ foam as a strategy for enhancing the therapeutic efficacy of a rectally administered GLP-2 analog. This approach improved colonic absorption and extended drug retention in the colon. Previous studies have demonstrated that CO_2 significantly enhances the permeation of macromolecules in the colon.[17] However, this enhancement was limited by molecular weight, with smaller molecules such as FD 4K exhibiting better transcolonic transport than larger molecules such as FD 40K. Thus, we loaded glepaglutide with a similar molecular weight as FD 4K. More importantly, GLP-2 analogs have shown both systemic therapeutic effects, such as the induction of mucosal healing,[18–20] and local responses in the colon.[8,9] This dual action underscores the need for formulations capable of achieving both systemic and localized concentrations of the therapeutic agent, and the foam formulation could be optimized to fulfill this purpose.

To the best of our knowledge, very few studies have explored the noninvasive administration of GLP-2 analogs to treat colitis.[15,16] In this study, we investigated rectal administration as a potential delivery method. Interestingly, our locally delivered GLP-2 analogs demonstrated a therapeutic effect comparable to that of previously reported orally delivered GLP-2 analogs. For example, our rectal administration strategy achieved an even more pronounced decrease in colitis cytokines in tissue compared to previous reports in which orally administered nanoparticles were used.[16] Although there are some differences in experimental settings, these findings suggest that rectal administration could represent an efficient and promising strategy for delivering GLP-2 analogs.

Although the α-helix structure of GL is significantly disrupted by the gassing process (Figure 1C), GL maintains its therapeutic efficacy despite changes in its secondary structure. This finding was validated by our in vivo results, where GL demonstrated both anti-inflammatory effects in acute colitis model mice and intestinotrophic effects (Figures 3 and 4). These findings align with previous studies indicating that a reduction in the α-helical conformation of GLP-2 has a minimal effect on its therapeutic efficacy.[21] Substitution at Gly4, which altered the α-helix propensity, had a minimal effect on the binding of GL to GLP-2R.[21] Notably, although GL can also activate GLP-1R with low binding affinity,[22] this interaction is highly dependent on the secondary structure and is not further discussed in this manuscript because of the loss of secondary structure.[21] Conversely, despite the loss of secondary structure, the quaternary structure of GL remains intact postfoaming, as indicated by intrinsic fluorescence (Figure 2B). Intrinsic fluorescence analysis, which leverages the properties of fluorophore residues in certain amino acids, was employed to assess structural integrity. Tryptophan (Trp) is the amino acid responsible for protein fluorescence and has the

highest fluorescence quantum yield.[23] GL contains only one tryptophan residue at position 25, and the results indicate that the formulation did not cause structural changes at this site. Rather than suggesting an unchanged conformational structure for the entire peptide, the findings specifically point to the preservation of structural integrity at this particular residue. However, intrinsic fluorescence cannot fully interpret the conformational structure at other sites.

The foaming process did not cause GL degradation. Additionally, we attempted to load teduglutide (Ted), another GLP-2 analog, into the foam formulation. However, Ted degraded after the foaming process (Figure S3, Supporting Information). To establish foam as a universal platform for macromolecules, further modifications should be explored, such as adding other excipients to stabilize the peptides or adjusting the composition of the existing formulation.

GLP-2 and its analogs have demonstrated therapeutic effects in previous publications on colitis animal models,[8,15,24] but it has not been formulated for local delivery. A significant finding in our study was that locally administered GL (GLS), even with minor absorption, demonstrated an anti-inflammatory effect by reducing inflammatory cytokine levels (Figure 3). However, the local effect alone was insufficient to fully alleviate colitis, necessitating a combination of local and systemic effects for therapeutic efficacy. Furthermore, although an effervescent formulation is known to enhance the absorption of macromolecules by the colon[17] and has been validated by the induction of systemic effects (Figure 4), it has demonstrated less pronounced therapeutic efficacy, potentially due to its shorter retention time in the colon. The comparable therapeutic effect of GLF to that of GLsc can be attributed to three factors. First, the GLF delivers a high concentration of GL directly to the inflamed site. Second, the foaming excipients provide prolonged peptide retention in the colon. Third, the foam formulation improves the absorption of macromolecules in the colon, as deduced from the FD4K results (Figure 5). In summary, foaming excipients are crucial for enhancing therapeutic effects due to their potential to increase drug retention in the colon, with CO_2 in the formulation possibly acting as a permeation enhancer.

Citrulline, which is produced by enterocytes in the small intestine, is a biomarker for mucosal healing. The interaction between GL and GLP-2R enhances nitric oxide (NO) production in enterocytes,[25,26] which subsequently increases citrulline levels.[27] Unlike GLS, GLF and GLE induced a similar increase in citrulline in the DSS model that was comparable to that of GLsc (Figure 5). These findings suggested that these formulations could enhance the absorption of GL and trigger GLP-2R. Moreover, citrulline has been reported to exert a protective effect on inflamed tissue,[28] and increased citrulline further contributes to improved colon conditions.

The ratio of villus height to crypt depth is often used as a marker to indicate improved absorption. In some studies, increased villus height and shallower crypt depth reflected a better absorption site.[29] However, GLP-2 analogs can increase both villus (V) height and crypt (C) depth,[30] alleviating the change in the V/C ratio after treatment. GLsc-treated mice presented an increased V/C ratio in the jejunum (Figure S4, Supporting Information).

In previous studies, ex vivo experiments demonstrated significantly greater permeation with an effervescent-like formulation (foam without foaming excipient) than with a foam formulation.[17] However, our findings indicated that, compared with foam, the effervescent-like system did not further increase the FD 4K plasma concentration in vivo. This discrepancy could be explained by the differences in experimental conditions. Specifically, the ex vivo study utilized an "airtight" closed system, whereas the actual colon environment was more open. Permeation enhancement induced by CO_2 is a transient effect, which is consistent with our previous findings that reported no damage to the epithelium. These findings suggest that CO_2 could open tight junctions without breaching the colon mucosa and holds significant potential as a local permeation enhancer for macromolecules.

4. Conclusion

We incorporated a GLP-2 analog, GL, into a foam formulation. To assess its therapeutic effect, GL was administered locally in a colitis mouse model via three different formulations, and the results revealed that GL had a positive effect on alleviating colitis. Interestingly, the gas-containing formulation also promoted an intestinotrophic effect, suggesting enhanced local absorption. Among the tested formulations, GLF had the most pronounced therapeutic effect on colitis in mice, with results comparable to those from systemically administered GL. Notably, both the foam and effervescent-like formulations enhanced permeation to a similar extent, although the latter demonstrated a less effective therapeutic outcome. This permeation effect was transient and quickly reversible in the mice. However, further research is needed to improve the stability of macromolecules in foam formulations.

5. Experimental Section

Materials: Phosphate buffered saline (PBS) tablets and Dulbecco's phosphate buffered saline (DPBS) (1x) were purchased from Gibco (Life Technologies Limited – Thermo Fisher Scientific, Paisley, United Kingdom). Potassium bicarbonate ($KHCO_3$), Tween 20, gelatin, citric acid (CA), dipotassium phosphate, hexadecyltrimethylammonium bromide (HTAB), sodium hydroxide (NaOH), sodium chloride (NaCl), *O*-dianisidine, tris-(hydroxymethyl)aminomethane hydrochloride (Tris HCl), guanidine chloride and fluorescein dextran 4K (FD4K) were all purchased from Sigma–Aldrich (Steinheim, Germany). Gelot 64 was a gift from Gattefossé (Saint-Priest Cedex, France). Silica nanoparticles were purchased from nanoComposix (Fortis Life Sciences, San Diego, California, United States). Glepaglutide was purchased from MedChemExpress (MCE) (Monmouth Junction, New Jersey, United States). The proinflammatory Panel 1 (mouse) kit used for the measurement of cytokine levels was purchased from Meso Scale Discovery (MSD) (Rockville, Idaho, United States). A mouse citrulline ELISA kit was purchased from MyBioSource, Inc. (San Diego, California, United States). The Pierce BCA protein assay kit, ethylenediaminetetraacetic acid (EDTA), and TRIzol were purchased from Thermo Fisher Scientific (Rockford, Illinois, United States). Isoflurane was purchased from Isoflutek (Alivira Laboratorios Karizoo S.A., Barcelona, Spain). Hydrogen peroxide was purchased from Emprove Essential (Darmstadt, Germany). Triton X-100 and ethanol were purchased from Carl Roth GmbH (Karlsruhe, Germany). Sodium dodecyl sulfate (SDS) was purchased from Bio-Rad Laboratories, Inc. (Hercules, California, United States). Sodium deoxycholic acid was purchased from Roche Diagnostics GmbH (Mannheim, Germany). Phosphatase inhibitor cocktail tablets were purchased from Roche Holding AG (Basel, Switzer-

land). Dextran sodium sulfate (DSS) with a molecular weight of 36 000–50 000 Da was purchased from MP Biomedicals (Eschwege, Germany) for the permeation recovery study, and from Tdb Labs. (Uppsala, Sweden) for the foam in vivo efficacy study.

Preparation and Characterization of GLF: Separate acidic and basic preformulation solutions were prepared. To create the basic preformulation solution, PB was dissolved in PBS to yield a 2 M (200 g/L) concentration. GL was then dissolved at a concentration of 2 mg/mL. The preformulation solution was stored at 4 °C until use.

The acidic preformulation solution for GLF was prepared by mixing the emulsifiers (Gelot 64 and Tween 20) with the acidic solution. Gelot 64 was melted at 75 °C and homogeneously mixed with Tween 20 at a mass ratio of 1:5 to create an emulsifier mixture. The acidic solution was prepared by dissolving gelatin in 3 M citric acid in Milli-Q water at 75 °C under stirring at 200 rpm. This was followed by dilution with a silica nanoparticle solution (10 mg/mL in Milli-Q water) and additional Milli-Q water. The final citric acid solution (1 M) contained gelatin (200 mg/mL) and silica nanoparticles (3 mg/mL). The emulsifier mixture and the citric acid solution were then combined at a mass-to-volume ratio of 1:4 at 75 °C under stirring at 100 rpm to produce the acidic prefoam solution.

The expansion and stability of GLF were evaluated using a scaled Falcon tube. A total of 200 µL of acidic preformulation solution was combined with 200 µL of basic preformulation solution, with or without the inclusion of GL. The resulting foam was incubated in a 37 °C water bath, and the foam volume was recorded at 1 min intervals, with the maximum expansion volume noted. Foam stability was determined by measuring the time required for the foam to completely dissipate.

An effervescent formulation (GLE) was prepared for comparison using a method similar to that used for GLF, but without the addition of any foaming excipients to the acidic preformulation solution. Specifically, 0.8 M citric acid was used as the acidic pre-formulation solution for GLE. Both GLF and GLE utilized the same preformulation solution.

For both GLF and GLE, the acidic preformulation solution and the basic preformulation solution were mixed at a 1:1 volume ratio.

Impact of the Gassing Process on the Structure of GL: The impact of gassing on the structural changes of GL was studied using both intrinsic fluorescence and circular dichroism (CD). The structural changes after the gassing process were compared to those of the GL in basic preformulation solution (before gassing).

To prepare the samples, GL was dissolved in basic solution to a concentration of 2 mg/mL. Then, 50 µL of this basic preformulation solution was mixed with 50 µL of 0.8 M citric acid.

The conformational stability of GL was assessed via intrinsic fluorescence spectroscopy as previously described.[17,31] GL samples in the postgassing solution and in the preformulation solution were both diluted to 200 µg/mL. To prepare the unfolded GL, guanidine chloride (6 M) was used to dilute the GL to 200 µg/mL. The fluorescence spectra of the GL samples were then measured using a SpectraMax instrument (Molecular Device, USA) with an excitation wavelength of 280 nm and an emission wavelength ranging from 310 to 450 nm. The maximum emission wavelength of the GL in the postgassing solution was compared with that of the GL in the basic preformulation solution and the unfolded GL.

CD was used to measure changes in the secondary structure of the peptide. For this analysis, 400 µL of the prepared sample at a concentration of 200 µg/mL was loaded into a 1 mm quartz cuvette. The far-UV spectrum between 190 and 260 nm was recorded at room temperature using a circular dichroism spectropolarimeter (Biologic, France). The percentage of α-helix content was then calculated using the online BeStSel CD spectra analysis software.

Stability of GL During Foaming Process: GL degradation during the gassing process in GLF and GLE was quantified by measuring changes in the GL concentration using high-performance liquid chromatography (HPLC). For each formulation, 50 µL of the acidic phase and 50 µL of the basic phase were mixed in an Eppendorf tube. The mixtures were then incubated at 37 °C for 15 min. Subsequently, the formulations were diluted to 1 mL with PBS and centrifuged at 2000 x g for 10 min to remove bubbles. The supernatant was collected, and the concentration of GL was compared with that of GL in basic preformulation solution.

GL quantification was performed using a Shimadzu HPLC system equipped with a Kinetex 2.6 µm EVO C18 column (150 × 4.6 mm, 100 Å). The mobile phase consisted of acetonitrile (ACN) + 0.5% trifluoroacetic acid (TFA) and filtered ultrapure water + 0.5% TFA. The limit of detection was 4.44±0.43 µg/mL, and the limit of quantification was 13.31± 1.28 µg/mL.

In Vivo Study: All experimental protocols were approved by and performed in accordance with the local animal committee (2021/UCL/MD/030 and 2024/UCL/MD/020) and as specified by the Belgian Law of 29 May 2013 on the protection of laboratory animals.

In Vivo Murine Colitis Models: Seven-week-old male mice were purchased from Janvier Laboratories, France, and housed in a controlled environment (23 ± 2 °C, 12 h daylight cycle) with ad libitum access to food and sterile water. Dextran sodium sulfate (DSS) was used to induce acute murine colitis by administering DSS at a concentration of 3% in the drinking water for 5 days, with the solution replaced every other day (8 mice per group).[32] From Day 6 onward, fresh autoclaved water was provided, and the mice were euthanized on Day 8. The healthy control group received only autoclaved water throughout the experiment.

GLF, GLE, and GL solution (GLS) were administered rectally at a dose of 80 µg/mouse every other day (on Days 2, 6, and 8) to mice anesthetized with isoflurane. GL was also administered subcutaneously (GLsc) at a dose of 860 µg/kg following the same schedule. PBS was administered rectally to both healthy and DSS-treated mice as negative and positive controls, respectively. Foam without GL was administered as an additional comparison.

In Vivo Efficacy Evaluation: The weights of the mice were recorded daily, and weight loss was calculated as a percentage of the initial weight on day one. On the final day, the mice were anesthetized for colonoscopy imaging, and the severity of the disease was scored according to the criteria outlined in a previous publication.[33] Blood was collected from anesthetized mice via cardiopuncture. The intestines and colon were then harvested and dissected in different sections for further analysis.

The intestine was defined as the entire small intestine, from the duodenum to the ileum. The contents were gently removed, and the intestine weight was recorded. The jejunum and ileum were identified, and small sections of these organs were fixed in 4% formaldehyde for further analysis.

The cecum was excised from the colon, and the fecal contents were gently flushed out with PBS. The colon length was measured with a digital Vernier caliper, and the weight of each colon was recorded. The colon length-to-weight ratio was subsequently calculated. The colon was then sectioned into multiple pieces for further analysis.

To measure proinflammatory cytokines in the colon, tissue samples were frozen with liquid nitrogen and stored at -80 °C. For analysis, the colon was homogenized via a previously described method. The frozen dissected colon was weighed, and 150 mg of tissue per mL of cold lysis buffer (composed of 500 m MM NaCl, 2 m EDTA, 1% Triton X-100, 0.5% sodium deoxycholic acid, 0.1% SDS, cocktail protease inhibitor tablet, and 50 mM Tris-HCl in Milli-Q water) was added. The tissues were homogenized using a homogenizer (Bertin Technologies SAS, France) at 4000 × g for 15 s, at a 10 s, intervals for four cycles. The homogenate was then centrifuged at 100000 × g for 20 min. An aliquot of the supernatant (25 µL) was collected and analyzed for cytokine concentration in the tissue using a V-PLEX Plus Mouse Cytokine 19-Plex ELISA Kit (MesoScale Discovery, USA), following the manufacturer's instructions, and analyzed with a MESO QuickPlex SQ 120 plate reader (MesoScale Discovery, USA). The results were normalized to protein content, and quantified using a Pierce BCA protein assay kit.

To measure myeloperoxidase (MPO) levels in the colon, colon sections were frozen with liquid nitrogen and stored at -80 °C. Upon analysis, the colon was homogenized via a method similar to that previously described, with some modifications.[34] Specifically, a phosphate buffer (pH 6) with HTAB was used as the lysis buffer. A volume of 500 µL of lysis buffer was added to each piece of colon sample. The tissues were homogenized at 4000 × g for 15 s, with a 10 s interval, for four cycles. The homogenate was then centrifuged at 100 000 × g for 20 min. An aliquot of 7 µL of the supernatant was added to a 96-well plate to analyze MPO activity via

the addition of 200 µL of MPO analysis solution (phosphate buffer, pH 6, with 0.167 mg/mL *O*-dianisidine and 0.5 µL/mL H_2O_2). The plate was incubated at 37 °C for 5 min, and the absorbance at 460 nm was recorded using a SpectraMax iD5 multimode microplate reader. The results were normalized to the protein content and quantified with a Pierce BCA protein assay kit.

Plasma citrulline was measured with a mouse citrulline ELISA kit from MyBioSource (San Diego, USA).

Colon segments were initially fixed overnight in 4% buffered formalin for histological scoring, then sequentially washed with 70% ethanol and embedded in paraffin. These sections were subjected to hematoxylin–eosin (H&E) staining for histological evaluation, adhering to the histopathological criteria established by Koelink et al.[35]

The intestinotrophic effect of GL on the large intestine was evaluated by measuring the crypt depth and villus height. Sections of the ileum and jejunum were fixed overnight in 4% buffered formalin. The samples were then sequentially washed with 70% ethanol and embedded in paraffin. The sections were stained with Hematoxylin and eosin (H&E) stain. Crypt depth and villus height were measured via the software SlideViewer (3DHISTECH Soft, Hungary), and their ratios were also calculated.

Permeation Enhancement Effect of the Foam in Mice: FD 4K-loaded foam and effervescent formulations were prepared to evaluate their permeation effects. The acidic preformulation solution was prepared as described in Section Stability of GL During Foaming Process. The basic preformulation solution was prepared by dissolving FD 4K in a PB solution (2 M) at a concentration of 20 mg/mL.

Seven-week-old male mice were purchased from Janvier Laboratories, France, and housed in a controlled environment (23 ± 2 °C, 12 h daylight cycle) with ad libitum access to food and sterile water. Colitis was induced by adding DSS to the drinking water for 4 days. FD 4K-loaded foam (FDF), FD 4K-loaded effervescent formulation (FDE), and FD 4K solution (FDS) were rectally administered to the mice (8 mice per group). Blood samples were collected from the tail vein at 15 min and 1 h using capillaries. The blood was then centrifuged at 4000 × g for 14 min at 4 °C, and the plasma was retrieved. The concentration of FD 4K in the plasma was quantified by measuring the fluorescence intensity of FD 4K using a SpectraMax iD5 multimode microplate reader.

Healthy mice were used to evaluate the recovery of the permeation enhancement effect of the foam formulation. FDS and FDF were administered rectally to healthy mice. Blood samples were collected at 15 min and 1 h postadministration. In the other group, foam was administered first. After 4 h, FD 4K was administered. Blood was collected at 15 min and 1 h postadministration (5 mice per group). Blood samples were then centrifuged at 4000 × g for 14 min at 4 °C to obtain plasma. The FD 4K concentration in the plasma was quantified by measuring the fluorescence intensity of FD 4K via a SpectraMax iD5 multimode microplate reader.

Statistical Analysis: The statistical analysis in the study was performed using GraphPad Prism 9 software (USA). The Grubbs test was applied to identify and support the exclusion of any outliers in each group. Depending on the homogeneity of variance, as determined by the Brown–Forsythe test, either two-way or one-way ANOVA were utilized, followed by Tukey's post hoc test for multiple group comparisons. In cases where significant variance differences were observed between groups, a nonparametric analysis was conducted. For comparing two groups specifically, Student's t test was applied. The results were presented as the mean ± standard error of the mean (SEM). A *p* value (**p*) of less than 0.05 was set as the threshold for statistical significance.

Supporting Information

Supporting Information is available from the Wiley Online Library or from the author.

Acknowledgements

W.Z. is a research fellow from the F.R.S.-FNRS (Fonds de la Recherche Scientifique, FRIA). A.B. is a research associate from the Belgian FRS-FNRS (Fonds de la Recherche Scientifique) and a WEL Research Institute investigator. This work was supported by the FRS-FNRS (convention J.0010.20), FRFS-WELBIO, with the support of the Wallon region (under grant agreement WELBIO-CR-2022 S–01). The authors appreciate Rose-Marie Goebbels for her assistance in the histological study. Images have been created with Biorender.com.

Conflict of Interest

The authors declare no conflict of interest.

Author Contributions

W.Z., W.V.d.B., J.M., and A.B. performed conceptualization. W.Z., W.V.d.B., and A.B. performed methodology. W.Z. and A.B. performed the formal analysis. W.Z., W.V.d.B., H.Y., E.K.K., K.W., T.S., L.G., T.G.M., and A.B. conducted the investigation. W.Z. and A.B. wrote the original draft. W.Z., W.V.d.B., T.G.M., J.M., and A.B. reviewed and edited the writing. W.Z. and A.B. performed visualization. A.B. performed supervision, managed the administration, and acquired funding

Data Availability Statement

All data relevant to the study are included in the article or uploaded as supplementary information. Complementary data that support the findings of this study are available from the corresponding author, A.B., upon reasonable request.

Keywords

colon delivery, foam, gas permeation enhancer, glepaglutide, inflammatory bowel disease

Received: September 13, 2024
Revised: January 8, 2025
Published online: February 5, 2025

[1] D. Kounatidis, N. G. Vallianou, D. Tsilingiris, G. S. Christodoulatos, E. Geladari, T. Stratigou, I. Karampela, M. Dalamaga, *Curr. Nutr. Rep.* **2022**, *11*, 618.
[2] J. Lovshin, D. J. Drucker, *Regul. Pept.* **2000**, *90*, 27.
[3] N. Abdalqadir, K. Adeli, *Microorganisms* **2022**, *10*, 2061.
[4] B. Yusta, R. P. Boushey, D. J. Drucker, *J. Biol. Chem.* **2000**, *275*, 35345.
[5] S. Xie, B. Liu, S. Fu, W. Wang, Y. Yin, N. Li, W. Chen, J. Liu, D. Liu, *Cell. Physiol. Biochem.* **2014**, *34*, 590.
[6] Y. Feng, F. R. Demehri, W. Xiao, Y.-H. Tsai, J. C. Jones, C. D. Brindley, D. W. Threadgill, J. J. Holst, B. Hartmann, T. A. Barrett, D. H. Teitelbaum, P. J. Dempsey, *Cell Mol. Gastroenterol. Hepatol.* **2017**, *3*, 447.
[7] W. Zhang, C. B. Michalowski, A. Beloqui, *Front. Bioeng. Biotechnol.* **2021**, *9*, 675194.
[8] J. Gu, J. Liu, T. Huang, W. Zhang, B. Jia, N. Mu, K. Zhang, Q. Hao, W. Li, W. Liu, W. Zhang, Y. Zhang, X. Xue, C. Zhang, M. Li, *Biochem. Pharmacol.* **2018**, *155*, 425.
[9] D. Li, Y. Yang, X. Yin, Y. Liu, H. Xu, Y. Ni, P. Hang, S. Niu, H. Zhang, W. Ding, H. Kuang, *Bioengineered* **2021**, *12*, 5195.
[10] B. Hartmann, M. B. Harr, P. B. Jeppesen, M. Wojdemann, C. F. Deacon, P. B. Mortensen, J. J. Holst, *J. Clin. Endocrinol. Metab.* **2000**, *85*, 2884.
[11] M. P. DaCambra, B. Yusta, M. Sumner-Smith, A. Crivici, D. J. Drucker, P. L. Brubaker, *Biochemistry* **2000**, *39*, 8888.

[12] R. M. Naimi, M. Hvistendahl, L. H. Enevoldsen, J. L. Madsen, S. Fuglsang, S. S. Poulsen, H. Kissow, J. Pedersen, N. Nerup, R. Ambrus, M. P. Achiam, L. B. Svendsen, J. J. Holst, B. Hartmann, S. H. Hansen, L. O. Dragsted, A. Steensberg, U. Mouritzen, M. B. Hansen, P. B. Jepppesen, *Lancet Gastroenterol Hepatol.* **2019**, *4*, 354.
[13] M. A. Agersnap, K. Sonne, K. M. Knudsen, C. B. Knudsen, M. Berner-Hansen, *Clin. Microbiol. Infect.* **2022**, *42*, 1093.
[14] P. B. Jeppesen, T. Vanuytsel, S. Subramanian, F. Joly, G. Wanten, G. Lamprecht, M. Kunecki, F. Rahman, T. S. Nielsen, L. B. Graff, M. Berner-Hansen, U. F. Pape, D. F. Mercer, *Transplantation* **2023**, *107*, 39.
[15] V. Marotti, Y. Xu, C. Bohns Michalowski, W. Zhang, I. Domingues, H. Ameraoui, T. G. Moreels, P. Baatsen, M. Van Hul, G. G. Muccioli, P. D. Cani, M. Alhouayek, A. Malfanti, A. Beloqui, *Bioact. Mater.* **2024**, *32*, 206.
[16] A. S. Barros, S. Pinto, J. Viegas, C. Martins, H. Almeida, I. Alves, S. Pinho, R. Nunes, A. Harris, B. Sarmento, *Small* **2024**, *20*, 2402502.
[17] W. Zhang, F. McCartney, Y. Xu, C. B. Michalowski, I. Domingues, E. K. Kambale, T. G. Moreels, L. Guilbaud, C. Chen, V. Marotti, D. J. Brayden, A. Beloqui, *J. Control. Release* **2024**, *374*, 254.
[18] H. A. Redstone, W. D. Buie, D. A. Hart, L. Wallace, P. J. Hornby, S. Sague, J. J. Holst, D. L. Sigalet, *Gastroenterol. Res. Pract.* **2010**, *2010*, 672453.
[19] K. Bulut, J. J. Meier, N. Ansorge, P. Felderbauer, F. Schmitz, P. Hoffmann, W. E. Schmidt, B. Gallwitz, *Regul. Pept.* **2004**, *121*, 137.
[20] M. Kjaer, W. Russell, P. Schjerling, E. Cottarelli, K. N. Christjansen, D. M. G. Olsen, P.-M. Krarup, L. Jessen, M. Berner-Hansen, L. N. Jorgensen, M. S. Ågren, *Gastroenterol. Res. Pract.* **2020**, *2020*, 8460508.
[21] R. Gibadullin, B. P. Cary, S. H. Gellman, *J. Am. Chem. Soc.* **2023**, *145*, 12105.
[22] D. M. Hargrove, S. Alagarsamy, G. Croston, R. Laporte, S. Qi, K. Srinivasan, J. Sueiras-Diaz, K. Wisniewski, J. Hartwig, M. Lu, A. P. Posch, H. Wisniewska, C. D. Schteingart, P. J.-M. Rivière, V. Dimitriadou, *J. Pharmacol. Exp. Ther.* **2020**, *373*, 193.
[23] V. V. Khrustalev, V. V. Poboinev, A. N. Stojarov, T. A. Khrustaleva, *Eur. Biophys. J.* **2019**, *48*, 523.
[24] D. Li, Y. Gao, L. Cui, Y. Li, H. Ling, X. Tan, H. Xu, *Front. Microbiol.* **2023**, *14*, 1174308.
[25] E. M. Grande, F. Raka, S. Hoffman, K. Adeli, *Diabetes* **2022**, *71*, 1388.
[26] K. Mukherjee, C. Xiao, *Front. Physiol.* **2024**, *15*, 1358625.
[27] A. M. Gonzalez, E. T. Trexler, *J. Strength Cond. Res.* **2020**, *34*, 1480.
[28] B. Cai, M.-H. Zhou, H.-L. Huang, A.-C. Zhou, Z.-D. Chu, X.-D. Huang, C.-W. Li, *PLoS One* **2020**, *15*, e0240883.
[29] T. N. D. Nguyen, N. H. Le, V. V. Pham, P. Eva, F. Alberto, H. T. Le, *J. Agric. Dev.* **2021**, *20*, 1.
[30] M. R. Hellmich, B. M. Evers, in *Physiology of the Gastrointestinal Tract*, 4th (Ed: L.R. Johnson), Academic Press, Burlington **2006**, pp. 435–458.
[31] S. Mahri, T. Wilms, P. Hagedorm, M.-J. Guichard, K. Vanvarenberg, M. Dumoulin, H. Frijlink, R. Vanbever, *Eur. J. Pharm. Sci.* **2023**, *189*, 106522.
[32] S. Wirtz, V. Popp, M. Kindermann, K. Gerlach, B. Weigmann, S. Fichtner-Feigl, M. F. Neurath, *Nat. Protoc.* **2017**, *12*, 1295.
[33] C. Becker, M. Fantini, M. Neurath, *Nat. Protoc.* **2006**, *1*, 2900.
[34] M. Alhouayek, P. Bottemanne, K. V. Subramanian, D. M. Lambert, A. Makriyannis, P. D. Cani, G. G. Muccioli, *FASEB J.* **2015**, *29*, 650.
[35] P. J. Koelink, M. E. Wildenberg, L. W. Stitt, B. G. Feagan, M. Koldijk, A. B. van 't Wout, R. Atreya, M. Vieth, J. F. Brandse, S. Duijst, A. A. te Velde, G. R. A. M. D'Haens, B. G. Levesque, G. R. van den Brink, *J. Crohn's Colitis.* **2018**, *12*, 794.